PAPER

Engulfment control of platinum nanoparticles into oxidized silicon substrates for fabrication of dense solid-state nanopore arrays

View the article online for updates and enhancements.

IOP ebooks™

Bringing you innovative digital publishing with leading voices to create your essential collection of books in STEM research.

Start exploring the collection - download the first chapter of every title for free.

Engulfment control of platinum nanoparticles into oxidized silicon substrates for fabrication of dense solid-state nanopore arrays

Hai Le-The[1] , Corentin Tregouet[1,2], Michael Kappl[3], Maren Müller[3], Katrin Kirchhoff[3], Detlef Lohse[2], Albert van den Berg[1], Mathieu Odijk[1] and Jan C T Eijkel[1,4]

[1] BIOS Lab-on-a-Chip Group, MESA+ Institute for Nanotechnology, Max Planck Center for Complex Fluid Dynamics, University of Twente, The Netherlands
[2] Physics of Fluids Group, MESA+ Institute for Nanotechnology, Max Planck Center for Complex Fluid Dynamics, University of Twente, The Netherlands
[3] Max Planck Institute for Polymer Research, Mainz, Germany

E-mail: h.lethe@utwente.nl and j.c.t.eijkel@utwente.nl

Abstract

We found that platinum (Pt) nanoparticles, upon annealing at high temperature of 1000 °C, are engulfed into amorphous fused-silica or thermal oxide silicon substrates. The same phenomenon was previously published for gold (Au) nanoparticles. Similar to the Au nanoparticles, the engulfed Pt nanoparticles connect to the surface of the substrates through conical nanopores, and the size of the Pt nanoparticles decreases with increasing depth of the nanopores. We explain the phenomena as driven by the formation of platinum oxide by reaction of the platinum with atmospheric oxygen, with platinum oxide evaporating to the environment. We found that the use of Pt provides much better controllability than the use of Au. Due to the high vapor pressure of platinum oxide, the engulfment of the Pt nanoparticles into oxidized silicon (SiO_2) substrates is faster than of Au nanoparticles. At high temperature annealing we also find that the aggregation of Pt nanoparticles on the substrate surface is insignificant. As a result, the Pt nanoparticles are uniformly engulfed into the substrates, leading to an opportunity for patterning dense nanopore arrays. Moreover, the use of oxidized Si substrates enables us to precisely control the depth of the nanopores since the engulfment of Pt nanoparticles stops at a short distance above the SiO_x/Si interface. After subsequent etching steps, a membrane with dense nanopore through-holes with diameters down to sub-30 nm is obtained. With its simple operation and high controllability, this fabrication method provides an alternative for rapid patterning of dense arrays of solid-state nanopores at low-cost.

Supplementary material for this article is available online

(Some figures may appear in colour only in the online journal)

---

[4] Authors to whom any correspondence should be addressed.

Introduction

Solid-state nanopores have attracted much scientific interest due to their excellent properties including size-tunability, high reliability and stability, easy modification and integration [1–4]. Among potential applications in sensing [5], separation [6], purification [7, 8], solid-state nanopores are intensively used for DNA sequencing and protein detection [9–11]. Many methods have been reported to fabricate solid-state nanopores, which can be separated in two categories namely high-energy beam sculpting [12–14] and conventional manufacturing [15–20]. Although high-energy beam based methods can precisely produce nanopores in silicon nitride or silicon oxide with diameters down to approximately 1 nm, these methods are time- and labor-intensive, and require dedicated systems. Therefore, high-yield fabrication of solid-state nanopore arrays is not possible at low-cost. Conventional methods, for example mask etching [15, 17], nanoimprinting [16], electrical breakdown [19], offer a high production rate, but lack precise control of both reproducibility and pore dimensions. Surwade *et al* reported the fabrication of a nanoporous graphene film by using oxygen plasma etching of graphene [8]. Although nanopores with the diameter of 0.5–1 nm can be produced, this fabrication method is limited to graphene only. Therefore, a robust and simple fabrication method for high-yield patterning of dense arrays of solid-state nanopores at low-cost is necessary.

Recently, de Vreede *et al* reported the engulfment of Au nanoparticles into amorphous fused silica substrates at high temperature [21]. Annealing at approximately 1050 °C, Au nanoparticles are found to become engulfed perpendicularly into the substrates, leaving a nanopore connection to the substrate surface. Using this observed phenomenon, closed-end nanopores with diameters of approximately 25 nm, and lengths up to 800 nm were fabricated into amorphous fused-silica substrates. Although this proved a simple method for making solid-state nanopores through membranes [22], it is difficult to precisely control the uniformity in the engulfment depth of Au nanoparticles, or the dimension and uniformity of the nanopores. Moreover, the aggregation of Au nanoparticles at high temperature limits the use of this method for making dense arrays of solid-state nanopores.

In this paper, we report an alternative method to fabricate dense arrays of silicon oxide nanopores by annealing Pt nanodots supported directly on the surface of oxidized Si substrates at high temperature. The use of Pt nanoparticles leads to an opportunity for patterning dense nanopore arrays due to their insignificant aggregation at high temperature compared to Au nanoparticles. In addition, the use of oxidized Si substrates enables us to precisely control the depth of the nanopores since the engulfment of Pt nanoparticles stops above the SiO_x/Si interface. Using this combination with subsequent etching steps, we successfully demonstrate the fabrication of dense arrays of silicon oxide nanopore through-holes with diameters down to sub-30 nm

Materials and methods

Patterning dense arrays of Pt nanodots on thermally oxidized Si wafers

Figure 1 shows the fabrication process for patterning arrays of Pt nanodots supported on the surface of thermally oxidized ($\sim$100 nm thick SiO_2) 4 inch Si wafers (525 μm thick, Okmetic, Finland), without the use of additional adhesion layers. Briefly, ultraviolet (UV)-based displacement Talbot lithography (DTL, PhableR 100 C, Eulitha) was used to pattern periodic $\sim$300 nm diameter nanoholes with $\sim$400 nm pitch into a positive photoresist (PR) layer of 200 $\pm$ 1.5 nm thickness (PFI88 photoresist diluted 1:1 with propylene glycol methyl ether acetate (PGMEA), Sumitomo Chemical Co., Ltd). These nanoholes which were subsequently transferred at a 1:1 ratio into a bottom anti-reflection layer coating (BARC) layer of 187 $\pm$ 2 nm thickness (AZ BARLi II 200) by using nitrogen (N_2) plasma etching in a parallel plate reactive ion etching system (in-house built TEtske system, MESA+, NanoLab) at wafer-level, 13 mTorr, and 25 W for 8 min [23]. These PR/BARC nanoholes were then used as a template for the fabrication of Pt nanodots using a lift-off process. To improve the adhesion strength of Pt with SiO_2, the patterned wafer was treated with UV-ozone (PR-100 UV-ozone Photoreactor, UVP Inc.) for 5 min after the sputtering of a Pt layer using an ion-beam sputtering system (in-house built T'COathy system, MESA+, NanoLab) [24]. By performing the lift-off process in a 99% nitric acid (HNO_3) solution, dense arrays of Pt nanodots supported on the surface of oxidized Si wafers were obtained.

High temperature annealing of Pt nanodots on oxidized Si substrates

The fabricated Pt nanodots were annealed at high temperature by using a furnace (TSD-12 furnace, Toma, Netherlands) in environmental air. Different annealing recipes were conducted to investigate the effects of the annealing temperature and time on the dewetting of Pt nanodots into Pt nanoparticles, and the engulfment of the Pt nanoparticles into the oxidized Si substrates. It is worth to mention that the furnace was closed completely during the annealing processes.

Manufacturing membranes with dense arrays of sub-30 nm nanopores

Figure 2 show the fabrication process for manufacturing membranes with dense arrays of through-hole sub-30 nm nanopores, using the prior engulfment of Pt nanoparticles into an oxidized Si substrate. Briefly, an oxidized Si substrate containing engulfed Pt nanoparticles (figure 2(a)) was wet etched in a 25% potassium hydroxide (KOH) solution at 75 °C, to selectively remove the bulk Si from the backside (figure 2(b)). Thereafter, a dry etching process of SiO_2 was conducted from the backside of the sample in a parallel plate reactive etching system (in-house built TEtske system, MESA+, NanoLab)
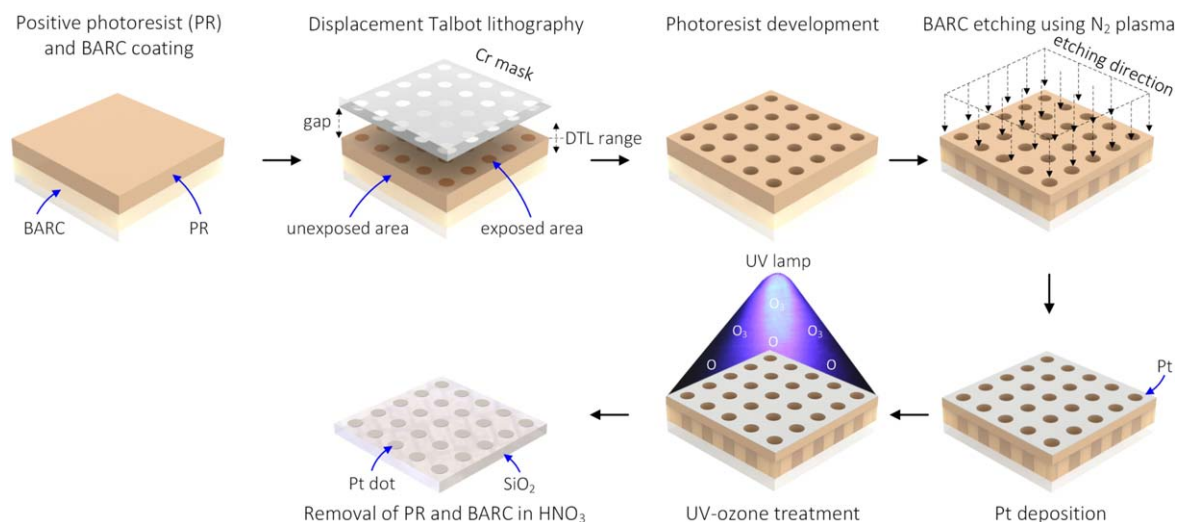
Figure 1. Fabrication process for patterning Pt nanodots (∼300 nm diameter, ∼400 nm pitch) supported directly on the surface of oxidized Si wafers, combining DTL with a lift-off process.
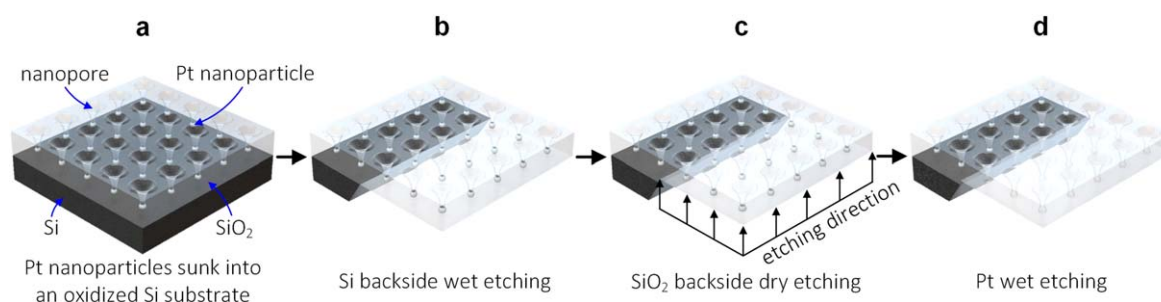

Figure 2. Fabrication process for patterning dense arrays of through-hole sub-30 nm nanopores. (a) Pt nanoparticles engulfed into an oxidized Si substrate upon annealing at high temperature. (b) Wet etching of the bulk Si substrate, and subsequently (c) dry etching of the SiO_2 layer from the backside. (d) Wet etching of Pt nanoparticles to open the through-hole nanopores.

using a mixture plasma of 25 sccm fluoroform (CHF_3) and 5 sccm oxygen (O_2) at 10 mTorr, and 60 W for 1 min and 30 s, to thin down the SiO_2 layer to reach the Pt nanoparticles (figure 2(c)). Subsequent etching of the sample in a mixture solution of 30% HNO_3 and 27% hydrochloric acid (HCl) at a ratio of 1:9:20 –HNO_3:HCl:H_2O at 90 °C, for 10 min, resulted in a removal of the Pt nanoparticles, thus opening the nanopores (figure 2(d)).

Characterization

High resolution scanning electron microscope (HR-SEM) images were captured by using a FEI Sirion microscope at a 5 kV acceleration voltage and a spot size of 3. The surface topography of structures was measured by using an atomic-force microscopy (Dimension Icon, Bruker Corp.) in contact mode in air. The thickness of the sputtered Pt layers and the SiO_2 layers was measured by using an ellipsometer system (M-2000UI, J A Woollam Co.) at an angle of 75°. Sample for transmission electron microscopy (TEM) was prepared by using a focused ion beam (FIB) system (FEI Nova 600 NanoLab FIB). The TEM specimen was measured by using a TEM system (FEI Tecnai F20) at a 200 kV acceleration voltage.

Results and discussion

Patterning dense arrays of Pt nanodots on oxidized Si substrates

Figure 3 shows the HR-SEM images of periodic Pt nanodots supported on the surface of an oxidized Si wafer, without additional adhesion layers. The top-view HR-SEM image shows a well-fabricated pattern of Pt nanodots (400 nm pitch) of approximately 300 nm in diameter (figure 3(a)). It is remarkable that all the Pt nanodots remained on the substrate surface after the lift-off process in the HNO_3 solution, thus indicating a good adhesion of Pt to SiO_2 obtained after treating the patterned wafer with UV-ozone for 5 min (see figure 1). The thickness of the sputtered Pt layer measured using the ellipsometer system was approximately 12.5 nm. The cross-sectional HR-SEM image shows residues of Pt at the edge of the patterned Pt nanodots (figure 3(b)). This phenomenon is typically encountered when using the lift-off process, and is caused by the sticking of unwanted metals deposited on the sidewall of PR patterns [25]. The fabricated Pt nanodot arrays were subsequently used to investigate the dewetting and engulfment process into the oxidized Si substrates by annealing at different temperatures.
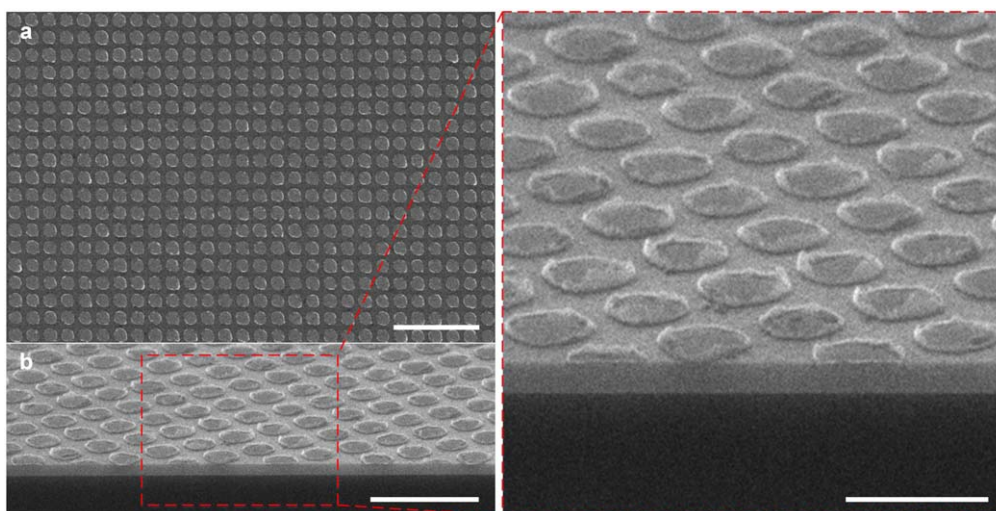
Figure 3. (a) Top-view (scale bar: 2 μm), and (b) cross-sectional (scale bar: 1 μm) HR-SEM images of periodic Pt nanodots supported directly on the surface of an oxidized Si wafer, with a close-up HR-SEM image (scale bar: 500 nm).
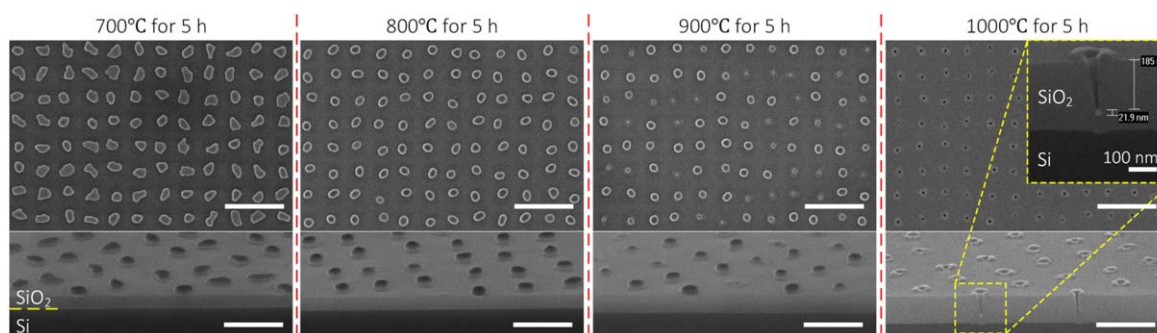

Figure 4. Top-view (scale bar: 1 μm) and cross-sectional (scale bar: 500 nm) HR-SEM images of Pt nanodots after annealing at different temperatures for 5 h. For all annealing processes, the ramp-up time was fixed at 2 h, and the furnace was passively cooled down to room temperature after heating.

High temperature annealing of Pt nanodots

Figure 4 shows the HR-SEM images of Pt nanodots after annealing at different temperatures, i.e. 700 °C, 800 °C, 900 °C, 1000 °C, for 5 h (figure S1, supporting information is available online at stacks.iop.org/NANO/30/065301/mmedia). It clearly shows that the shape and dimension of the Pt nanodots changed after annealing at 700 °C for 5 h, indicating Pt mobility and consequent dewetting at this relatively low temperature (700 °C) when compared to the melting temperature of Pt (~1768 °C). Such dewetting of Pt nanodots on SiO$_2$ surfaces at low temperature has been reported in literature [26]. Increasing the annealing temperature to 800 °C resulted into Pt nanoparticles with a more hemispherical shape. However, annealing at 900 °C for 5 h led to a significant reduction in the Pt nanoparticle circumference (figures S2 and S3, supporting information). We attribute this to the evaporation of platinum oxide via the oxidation of platinum at this temperature (900 °C) [27, 28]. Figure 5 shows that these Pt nanoparticles started to become engulfed into the SiO$_2$ layer, though at a relatively low uniformity. Several Pt nanoparticles were found to be completely engulfed, whereas other Pt nanoparticles had a ridge

formation of SiO$_2$ around their perimeter (figures S2 and S3, supporting information). Remarkably, these Pt nanoparticles were uniformly engulfed into the SiO$_2$ layer with only insignificant aggregation when compared to Au nanoparticles after annealing at 1000 °C for 5 h (figure S4, supporting information). Such a higher thermal stability of Pt nanoparticles compared to Au nanoparticles on SiO$_2$ substrates has also been observed by other investigators [29, 30]. By the engulfment, closed-end conical nanopores were formed in the SiO$_2$ layer with an end-diameter of sub-10 nm and a length of approximately 185 nm. It is noted that the thickness of the initial 100 nm thick SiO$_2$ layer further increased during the annealing process. Details of the proposed engulfment mechanism are given in the next section. It is worth to mention that the engulfment of all Pt nanoparticles stopped at a defined distance above the SiO$_x$/Si interface, thus leading to a precise control of the nanopore depth over large areas. This could be because the layer under the Pt nanoparticle is not fully oxidized to SiO$_2$ [31], or because stress is formed in this layer [32], which then leads to a decrease in the mobility of silicon oxide around the Pt nanoparticle surface. Both mechanisms could explain the termination of the engulfment of the Pt nanoparticle.
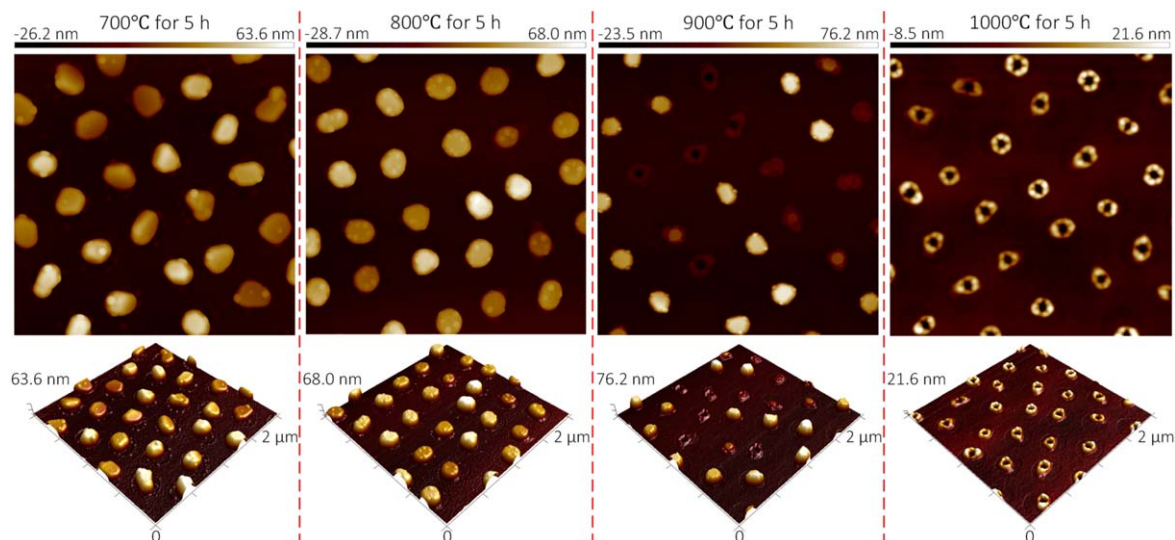
Figure 5. AFM (scan filed: 2×2 μm^2) images of Pt nanodots after annealing at different temperatures for 5 h.
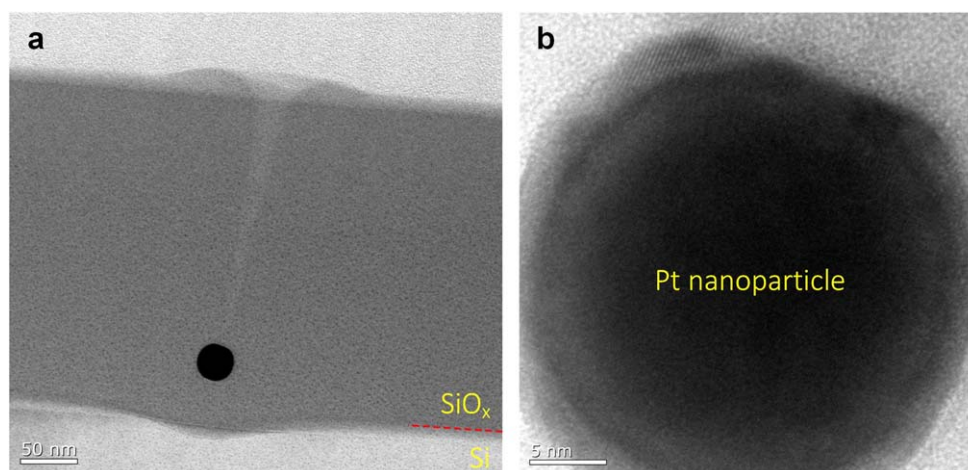

Figure 6. (a) Cross-sectional TEM images of a Pt nanoparticle engulfed into an oxidized Si substrate with (b) the corresponding close-up image of the Pt nanoparticle.

Mechanism of the engulfment of Pt nanoparticles in oxidized Si substrates

To investigate the engulfment mechanism of the Pt nano-particles into oxidized Si substrates, we measured the cross-section of an engulfed Pt nanoparticle connected to the sub-strate surface through a nanopore, using a TEM. A clear evidence of a flat crystal facet was observed at the upper side of the engulfed Pt nanoparticle (figure 6). A similar formation of crystal facets at the top of engulfed Au nanoparticles has been observed and reported by de Vreede *et al* [21]. In their paper, the engulfment of Au nanoparticles is attributed to the continuous evaporation of Au causing a constant change in the structural geometry, thus leading to the continuous migration of silica from below the Au nanoparticle to the triple line at its top in order to maintain equilibrium. As a result, the Au nanoparticle moves perpendicularly into the substrate. Assuming the Au evaporation was rate-limiting for the process, the engulfment depth as function of the annealing time could in good approximation be predicted [21]. This model did not include a description for the migration of silica along the nanoparticle, which process was recently modeled as driven by diffusiophoresis of Au in a nanometer thin vis-cous layer surrounding the Au nanoparticles [33]. We attri-bute the engulfment of Pt nanoparticles in oxidized Si substrates to comparable processes. It has to be noted that the platinum oxide evaporates faster than gold in atmospheric oxygen at high temperature as its vapor pressure is one order of magnitude higher than that of gold [34]. Further exper-imental verification is ongoing in order to confirm the relia-bility of the model, especially for the engulfment of Pt nanoparticles [35]. In addition, the influence of oxygen on the engulfment process can be further investigated by annealing the Pt nanoparticles in inert gases, i.e. N_2 or Ar.

In this paper, we apply the engulfment of Pt nanoparticles into oxidized Si substrates (figure 7) to fabricate dense arrays of through-hole sub-30 nm nanopores in a silicon oxide layer, combining wet etching and dry etching techniques (see next section).
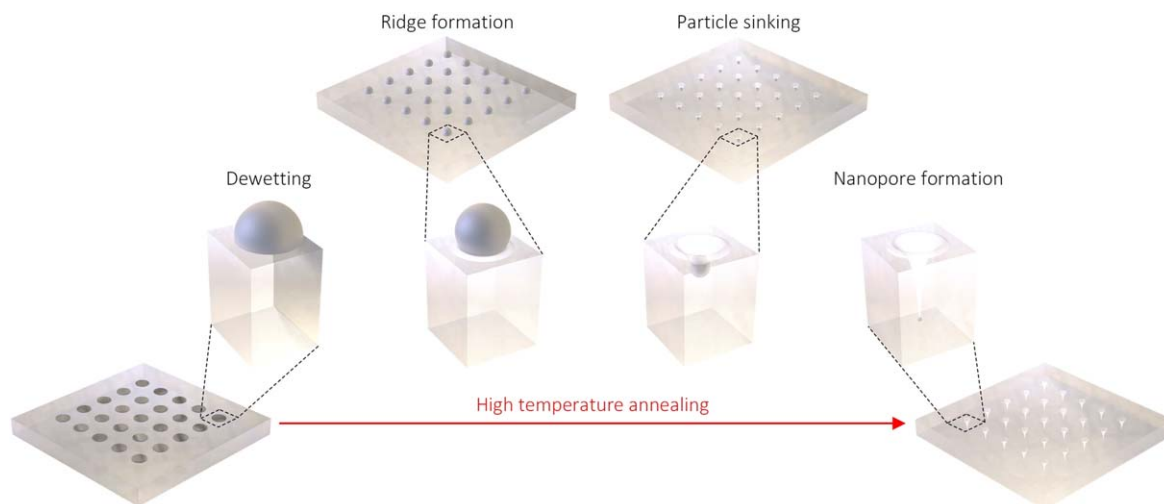
Figure 7. Formation of nanopores into oxidized Si substrates caused by the engulfment of Pt nanoparticles upon annealing at high temperature.
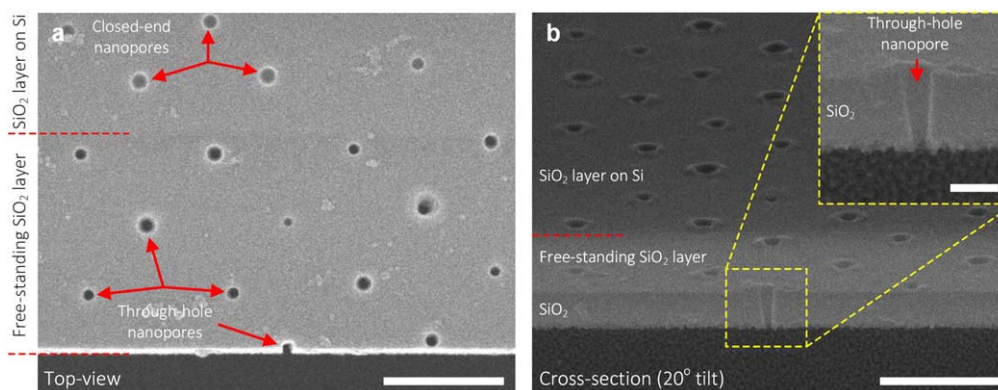

Figure 8. (a) Top-view (scale bar: 500 nm) and (b) cross-sectional (scale bar: 500 nm) HR-SEM images of periodic through-hole sub-30 nm nanopores created in a thick SiO_2 layer of approximately 160 nm, with a close-up image (scale bar: 100 nm).

Manufacturing membranes with dense arrays of sub-30 nm nanopores

Figure 8 shows HR-SEM images of an array of nanopores fabricated in a silicon oxide (SiO_2) layer of approximately 160 nm thickness. The top-view HR-SEM image (figure 8(a)) taken at the edge of the Si substrate (red dash line) shows a clear difference in the contrast between the through-hole nanopores (black) created into the free-standing SiO_2 area and the closed-end nanopores (gray). This indicates the success of the pore opening process from the backside of the SiO_2 layer (see figure 2). From the observation, almost all nanopores were opened (~95%). In addition, a well-ordered pattern of through-hole nanopores was obtained. The cross-sectional image (figure 8(b)) confirms the opening of the nanopores with diameters down to sub-30 nm (figure S5, supporting information). The average top-diameter of the nanopores was approximately 31.9 nm with a variation (standard deviation) of 6.5 nm. The through-hole nanopores have a conical shape due to the continuous evaporation of the Pt nanoparticles during the engulfment. Further optimization and timing of the etching processes, especially of the final SiO_2 dry etching step, is expected to produce through-hole nanopores of even

smaller end-diameters as the closed-end nanopores had end-diameters in the sub-10 nm range (figure S6, supporting information). Moreover, subsequent conformal deposition of a silicon nitride layer or an aluminum oxide layer can also probably reduce the nanopore diameter [10].

Conclusion

In summary, we report an alternative method to fabricate solid-state nanopores into oxidized Si substrates by annealing Pt nanodots supported directly on the substrate surface at high temperature. Compared to the previous approach using Au, we found that Pt nanoparticles were engulfed faster into the oxidized Si substrates, even though Pt has a higher melting temperature (~1768 °C) than Au (~1064 °C). We attribute this to the formation and subsequent evaporation of volatile platinum oxide in atmospheric environment. In addition, the aggregation of Pt nanoparticles was found to be insignificant compared to that of Au nanoparticles annealed at the same temperature, thus leading to an opportunity to pattern dense regular arrays of solid-state nanopores. Moreover, the use of oxidized Si substrates enables us to precisely control the

depth of the nanopores since the engulfment of Pt nanoparticles stops above the SiO_x/Si interface. Using the engulfment of Pt nanoparticles into oxidized Si substrates, we fabricated dense arrays of through-hole nanopores in a freestanding SiO_2 layer with sub-30 nm pore diameter. With its simple operation, our fabrication method provides an alternative for rapid patterning of dense arrays of solid-state nanopores at low-cost.

Acknowledgments

Competing interests

The authors declare no conflict of interest.

ORCID iDs

Hai Le-The https://orcid.org/0000-0002-3153-2937

References

[1] Dekker C 2007 Solid-state nanopores *Nat. Nanotechnol.* **2** 209–15

[2] Kudr J, Skalickova S, Nejdl L, Moulick A, Ruttkay-Nedecky B, Adam V and Kizek R 2015 Fabrication of solid-state nanopores and its perspectives *Electrophoresis* **36** 2367–79

[3] Deng T, Li M, Wang Y and Liu Z 2015 Development of solid-state nanopore fabrication technologies *Sci. Bull.* **60** 304–19

[4] Yuan Z, Wang C, Yi X, Ni Z, Chen Y and Li T 2018 Solid-state nanopore *Nanoscale Res. Lett.* **13** 1–10

[5] Shi W, Friedman A K and Baker L A 2017 Nanopore sensing *Anal. Chem.* **89** 157–88

[6] Prabhu A S, Jubery T Z N, Freedman K J, Mulero R, Dutta P and Kim M J 2010 Chemically modified solid state nanopores for high throughput nanoparticle separation *J. Phys.: Condens. Matter* **22** 454107

[7] Warkiani M E, Bhagat A A S, Khoo B L, Han J, Lim C T, Gong H Q and Fane A G 2013 Isoporous micro/nanoengineered membranes *ACS Nano* **7** 1882–904

[8] Surwade S P, Smirnov S N, Vlassiouk I V, Unocic R R, Veith G M, Dai S and Mahurin S M 2015 Water desalination using nanoporous single-layer graphene *Nat. Nanotechnol.* **10** 459–64

[9] Fanget A, Traversi F, Khlybov S, Granjon P, Magrez A, Forro L and Radenovic A 2014 Nanopore integrated nanogaps for DNA detection *Nano Lett.* **14** 244–9

[10] Liu Y and Yobas L 2016 Slowing DNA translocation in a nanofluidic field-effect transistor *ACS Nano* **10** 3985–94

[11] Farimani A B, Dibaeinia P and Aluru N R 2017 DNA origami-graphene hybrid nanopore for DNA detection *ACS Appl. Mater. Interfaces* **9** 92–100

[12] Li J, Stein D, McMullan C, Branton D, Aziz M J and Golovchenko J A 2001 Ion-beam sculpting at nanometre length scales *Nature* **412** 166–9

[13] Storm A J, Chen J H, Ling X S, Zandbergen H W and Dekker C 2003 Fabrication of solid-state nanopores with single-nanometre precision *Nat. Mater.* **2** 537–40

[14] Lo C J, Aref T and Bezryadin A 2006 Fabrication of symmetric sub-5 nm nanopores using focused ion and electron beams *Nanotechnology* **17** 3264–7

[15] Liang J, Chik H, Yin A and Xu J 2002 Two-dimensional lateral superlattices of nanostructures: nonlithographic formation by anodic membrane template *J. Appl. Phys.* **91** 2544–6

[16] Austin M D, Ge H, Wu W, Li M, Yu Z, Wasserman D, Lyon S A and Chou S Y 2004 Fabrication of 5 nm linewidth and 14 nm pitch features by nanoimprint lithography *Appl. Phys. Lett.* **84** 5299–301

[17] Whitney A V, Myers B D and Van D R P 2004 Sub-100 nm triangular nanopores fabricated with the reactive ion etching variant of nanosphere lithography and angle-resolved nanosphere lithography *Nano Lett.* **4** 1507–11

[18] James T, Kalinin Y V, Chan C C, Randhawa J S, Gaevski M and Gracias D H 2012 Voltage-gated ion transport through semiconducting conical nanopores formed by metal nanoparticle-assisted plasma etching *Nano Lett.* **12** 3437–42

[19] Kwok H, Briggs K and Tabard-Cossa V 2014 Nanopore fabrication by controlled dielectric breakdown *PLoS One* **9** e92880

[20] Deng T, Wang Y, Chen Q, Chen H and Liu Z 2016 Massive fabrication of silicon nanopore arrays with tunable shapes *Appl. Surf. Sci.* **390** 681–8

[21] De Vreede L J, Van Den Berg A and Eijkel J C T 2015 Nanopore fabrication by heating Au particles on ceramic substrates *Nano Lett.* **15** 727–31

[22] De Vreede L J, Muniz M S, Van Den Berg A and Eijkel J C T 2016 Nanopore fabrication in silicon oxynitride membranes by heating Au-particles *J. Micromech. Microeng.* **26** 037001

[23] Le-The H, Berenschot E, Tiggelaar R M, Tas N R, van den Berg A and Eijkel J C T 2017 Shrinkage control of photoresist for large-area fabrication of sub-30 nm periodic nanocolumns *Adv. Mater. Technol.* **2** 1600238

[24] Le-The H, Berenschot E, Tiggelaar R M, Tas N R, van den Berg A and Eijkel J C T 2018 Large-scale fabrication of highly ordered sub-20 nm noble metal nanoparticles on silica substrates without metallic adhesion layers *Microsyst. Nanoeng.* **4** 4

[25] Madou M J 2012 *Fundamentals of Microfabrication and Nanotechnology* 2nd edn (Boca Raton, FL: CRC press)

[26] Yu R, Song H, Zhang X F and Yang P 2005 Thermal wetting of platinum nanocrystals on silica surface *J. Phys. Chem. B* **109** 6940–3

[27] Jehn H 1981 Platinum losses during high temperature oxidation *J. Less-Common Met.* **78** 33–41

[28] Wrbanek J D and Laster K L H 2005 Preparation and analysis of platinum thin films for high temperature sensor applications *NASA* **19** 213433

[29] Eppler A S, Rupprechter G, Anderson E A and Somorjai G A 2000 Thermal and chemical stability and adhesion strength of Pt nanoparticle arrays supported on silica studied by transmission electron microscopy and atomic force microscopy *J. Phys. Chem. B* **104** 7286–92

[30] Veith G M, Lupini A R, Rashkeev S, Pennycook S J, Mullins D R, Schwartz V, Bridges C A and Dudney N J 2009 Thermal stability and catalytic activity of gold nanoparticles supported on silica *J. Catal.* **262** 92–101

[31] Kissinger G, Schubert M A, Kot D and Grabolla T 2017 Investigation of the composition of the Si/SiO_2 interface in

oxide precipitates and oxide layers on silicon by STEM/ EELS *ECS J. Solid State Sci. Technol.* **6** N54–63

[32] Fitch J T 1989 Intrinsic stress and stress gradients at the SiO$_2$/Si interface in structures prepared by thermal oxidation of Si and subjected to rapid thermal annealing *J. Vac. Sci. Technol.* B **7** 775

[33] Tregouet C B M, Le-The H, Odijk M, Snoeijer J, Eijkel J, Lohse D and van den Berg A 2017 Diffusiophoresis of gold in silica driven by the nanometric interfacial layer *21st Int. Conf. Miniaturized Syst. Chem. Life Sci.* pp 269–70

[34] Chaston J C 1975 Oxidation of the platinum metals *Platinum Met. Rev.* **19** 135–40

[35] Tregouet C B M, Le-The H, Kappl M, Müller M, Kirchhoff K, Odijk M, Snoeijer J H, van den Berg A, Lohse D and Eijkel J C T Surface osmotic flow and diffusiophoresis of gold nanoparticles in solid fused silica (unpublished)